San Jose State University
SJSU ScholarWorks

Faculty Publications

Meteorology and Climate Science

July 1997

An Analysis of Tropical Transport: Influence of the Quasi-biennial Oscillation

Eugene C. Cordero
NASA Goddard Space Flight Center, Greenbelt, Maryland, eugene.cordero@sjsu.edu

S. Randolph Kawa
NASA Goddard Space Flight Center, Greenbelt, Maryland

Mark R. Schoeberl
NASA Goddard Space Flight Center, Greenbelt, Maryland

Follow this and additional works at: https://scholarworks.sjsu.edu/meteorology_pub

Part of the Atmospheric Sciences Commons, Climate Commons, and the Meteorology Commons

Recommended Citation

An analysis of tropical transport: Influence of the quasi-biennial oscillation

Eugene C. Cordero

Universities Space Research Association, Atmospheric Chemistry and Dynamics, NASA Goddard Space Flight Center, Greenbelt, Maryland

S. Randolph Kawa and Mark R. Schoeberl

Atmospheric Chemistry and Dynamics, NASA Goddard Space Flight Center, Greenbelt, Maryland

Abstract. An analysis of over 4 years of Upper Atmosphere Research Satellite (UARS) measurements of CH_4, HF, O_3, and zonal wind are used to study the influence of the quasi-biennial oscillation (QBO) on constituent transport in the tropics. At the equator, spectral analysis of the Halogen Occultation Experiment (HALOE) and Microwave Limb Sounder (MLS) observations reveals QBO signals in constituent and temperature fields at altitudes between 20 and 45 km. Between these altitudes, the location of the maximum QBO amplitude roughly corresponds with the location of the largest vertical gradient in the constituent field. Thus, at 40 km where CH_4 and HF have strong vertical gradients, QBO signals are correspondingly large, while at lower altitudes where the vertical gradients are weak, so are the QBO variations. Similarly, ozone, which is largely under dynamical control below 30 km in the tropics, has a strong QBO signal in the region of sharp vertical gradients (~28 km) below the ozone peak. Above 35 km, annual and semi-annual variations are also found to be important components of the variability of long-lived tracers. Therefore, above 30 km, the variability in CH_4 and HF at the equator is represented by a combination of semiannual, annual, and QBO timescales. A one-dimensional vertical transport model is used to further investigate the influence of annual and QBO variations on tropical constituent fields. QBO-induced vertical motions are calculated from observed high resolution Doppler imager (HRDI) zonal winds at the equator, while the mean annually varying tropical ascent rate is obtained from the Goddard two-dimensional model. Model simulations of tropical CH_4 confirm the importance of both the annual cycle and the QBO in describing the HALOE CH_4 observations above 30 km. Estimates of the tropical ascent rate and the variation due to the annual cycle and QBO are also discussed.

1. Introduction

The quasi-biennial oscillation (QBO) is the primary mode of variability in the tropical lower stratosphere and has been studied extensively using observations and models [e.g., *Reed et al.*, 1961; *Veryard and Ebdon*, 1961; *Angell and Korshover*, 1970; *Dunkerton*, 1985; *Takahashi and Boville*, 1992]. Zonal wind observations over the last four decades show a QBO amplitude of about 20 m/s and an oscillation period that varies from 21 to 36 months [*Naujokat*, 1986]. The wind regimes descend with time at a rate of approximately 1 km/month and are confined to the equatorial latitudes. The easterly winds typically have stronger magnitudes (30 m/s) and persist longer at higher altitudes; the westerly winds have weaker magnitudes (10 m/s) and persist longer at lower elevations [*Andrews et al.*, 1987]. The generation and maintenance of the QBO is believed to be due to the mechanical and thermal dissipation of vertically propagating equatorial waves [*Lindzen and Holton*, 1968; *Holton and Lindzen*, 1972].

A temperature QBO has also been observed in the tropical latitudes [*Reed*, 1964; *Nastrom and Belmont*, 1975; *Dunkerton and Delisi*, 1985]. The generation and characteristics of this oscillation can be largely explained by considering that the thermal wind relationship is valid even near the equator. Thus, in the vertical shear zones of the zonal wind QBO, temperature anomalies with an amplitude of 2-3 K are observed in the tropics [*Andrews et al.*, 1987].

Associated with the tropical temperature anomalies is a meridional circulation pattern in the tropics and subtropics [*Reed*, 1964; *Plumb and Bell*, 1982]. For example, a positive vertical wind shear (increasing westerlies with increasing height) at the equator will produce a warm anomaly at the equator and a cold anomaly in the subtropics. These temperature anomalies will be damped by radiative processes in a number of weeks; thus their existence can only be maintained by a circulation pattern that produces downward motion in the tropics (adiabatic warming) and upward motion in the subtropics (adiabatic cooling). A corresponding horizontal component connects this circulation cell, producing equatorward motion aloft and poleward motion at the lower levels. This residual circulation, which maintains the QBO-induced temperature anomaly, should have a direct effect on constituent fields in the tropics.

A number of studies have examined the influence of the QBO on stratospheric constituents in the tropics. In particular,

QBO signals in total ozone have been observed both in the tropics and extratropics for over three decades [*Funk and Garnham*, 1962; *Angell and Korshover*, 1973; *Oltmans and London*, 1982; *Hasebe*, 1984; *Lait et al.*, 1989; *Hollandsworth et al.*, 1995; *Randel and Wu*, 1996]. *Ling and London* [1986] used a one-dimensional model to show that the ozone QBO is due to vertical advection in the lower stratosphere and to temperature dependent photochemistry in the upper stratosphere. Because ozone is under photochemical control above about 28 km in the tropics, only a few studies have been able to examine QBO-induced transport above 30 km. These include observations of a sunset NO_2 QBO using data from the Stratospheric Aerosol and Gas Experiment II (SAGE II) instrument [*Zawodny and McCormick*, 1991; *Chipperfield et al.*, 1994]. Although QBO signals in other constituent fields are expected to be present, the lack of any long time period observations of these chemical species has precluded their detection.

Instruments onboard the Upper Atmosphere Research Satellite (UARS) have been making continuous observations of various chemical and dynamical fields since November 1991. These measurements can be used to study the annual and interannual variability of tropical constituent fields. The purpose of this paper is to study how the QBO and seasonal cycle influence constituent transport in the tropics using both UARS observations and a simple vertical transport model. In this study we will use observations of temperature by the microwave limb sounder (MLS); methane (CH_4), hydrogen fluoride (HF), and ozone (O_3) by the Halogen Occultation Experiment (HALOE), and zonal wind by the high resolution Doppler imager (HRDI). Because CH_4 and HF are considered long-lived tracers throughout the stratosphere, their variability will be a valuable aid to better understanding transport processes in the middle and upper tropical stratosphere. Although the QBO has both meridional and vertical influences on constituent fields, this study will focus on how the QBO and annual cycle influence the vertical transport of constituents in the tropical stratosphere.

2. Observational Data

The UARS instrument HALOE uses a solar occultation sounding technique in the infrared to obtain vertical profiles of various constituents [*Park and Russell*, 1994]. From late 1991, HALOE has made nearly continuous measurements in the stratosphere and mesosphere during daily sunrises and sunsets. This observing pattern means that near-global coverage by HALOE is obtained in about a month. In this study, we use HALOE Version 18 data between 100 hPa and 1 hPa to construct time series of CH_4, HF, and O_3 from April 1992 through June 1996 in the tropical latitudes. In the tropical stratosphere, HF and O_3 data are accurate to better than 20% [*Russell et al.*, 1996; *Brühl et al.*, 1996] while the CH_4 data have an accuracy better than 15% [*Park et al.*, 1996]. The data profiles are zonally averaged and organized into 8° latitude bins centered about the equator. A trend of +6%/year, estimated from both models and observations [*Jackman et al.*, 1997] has been removed from the HF data. The presence of volcanic aerosols deposited by the eruption of Mount Pinatubo in June 1991 affected the HALOE retrievals in the lower stratosphere through the early part of 1992 [*Brühl et al.*, 1996]; thus we start our data analysis in March 1992.

UARS MLS temperature data (Version 3) are used to construct time series from November 1991 through June 1996. We use daily MLS temperatures from 100 hPa to 1 hPa between 4°S and 4°N, which have an accuracy of better than 3.5 K [*Fishbein et al.*, 1996]. MLS retrievals below 22 hPa (in altitude) are not scientifically useful; thus the MLS data set uses National Centers for Environmental Prediction (NCEP) analysis below this level [*Fishbein et al.*, 1996]. Because HALOE temperatures below 45 km rely heavily on NCEP analyzed temperature fields [*Hervig et al.*, 1996], these data are not used in this study.

Zonal wind data are obtained from HRDI. The stratospheric wind measurements are taken between 10 and 40 km in altitude and have a vertical resolution of 2.5 km. The horizontal resolution is about 500 km, and in this study, zonal means are constructed in monthly averaged, 2.5° latitude bins [*Ortland et al.*, 1996].

3. Zonal Wind and Temperature QBO

The HRDI wind instrument on board the UARS has been measuring global wind fields in the stratosphere (10-40 km) since November 1991. Figure 1 shows a time-height cross section of zonally averaged zonal winds over the equator. A recent comparison of the HRDI zonal winds with radiosonde observations in the tropics shows good overall agreement [*Ortland et al.*, 1996]. Timing and location of the wind regimes are well collocated, although the HRDI representation of the QBO shows weaker amplitudes and weaker vertical shear zones than seen in the radiosonde observations, a likely result of the lower HRDI vertical resolution.

Apparent in the HRDI observations are some of the known characteristics of the zonal wind QBO. The absolute magnitude of the easterly winds reaches 30 m/s, while the westerly winds generally reach 10 m/s. Between 20 and 35 km, the shear zones of the westerly winds appear to descend faster than the easterly regimes. Below about 20 km, the strength of the QBO amplitude drops off rapidly, and although the descending QBO is apparent, shorter period features are also present. Between 35 and 40 km, the semi-annual oscillation (SAO) appears to be superimposed on the QBO. For example, from January 1993 through April 1994, the magnitude of the easterly QBO winds present from 35 to 40 km are modulated by an apparent semiannual variation.
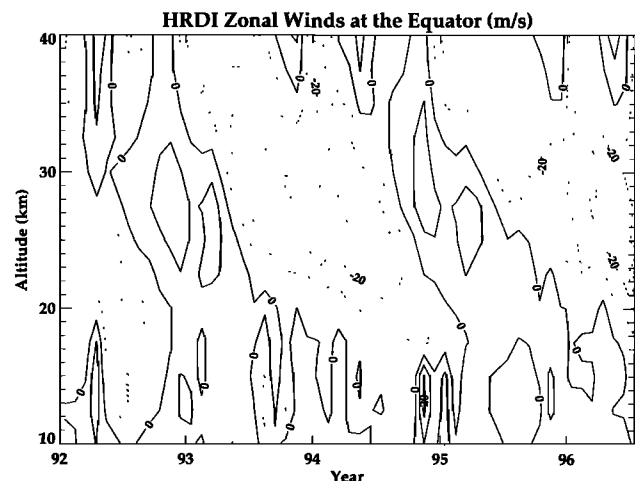

HRDI Zonal Winds at the Equator (m/s)

Figure 1. Time-height cross section of HRDI zonal winds centered over the equator. Contour interval is 10 m/s.
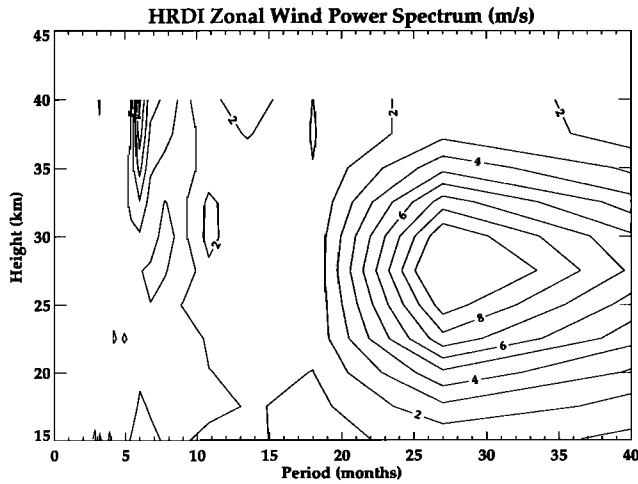
Figure 2. Amplitude of the HRDI zonal wind power spectra over the equator. Contour interval is 1 m/s.

A power spectrum analysis of the HRDI wind data is computed to investigate the dominant modes of variability found in the observations. The data are first interpolated onto regular time intervals, and then power spectra are obtained by computing the amplitude of the discrete complex Fourier transform of the time series.

Figure 2 shows the power spectrum of the HRDI zonal wind time series. The prominent feature is the large amplitudes seen between 18 and 38 km in the 27-month period range. Note that because the sample length is 54 months, the first two harmonics the Fourier analysis can resolve are 54 months and 27 months, respectively. The observed QBO during the UARS period had an average period close to 27 months (see Figure 1); thus the 27-month Fourier period should contain most of the QBO variation and will hereafter be associated with the QBO. The maximum amplitude of the QBO is 10 m/s at about 28 km. From 35 to 40 km, amplitudes of the annual and semiannual frequencies are about as large as the QBO frequency, in agreement with the rocketsonde observations of *Angell and Korshover* [1970].

Plate 1 shows the MLS zonal mean temperature deviation from 1992 through the middle of 1996 (the superimposed black contours are the reconstructed MLS temperatures, which will be discussed later). The maximum amplitude temperature deviation is around 4 K, with slightly larger values found above 35 km. From 25 to 30 km, the alternating warm and cold anomalies correspond with the westerly and easterly shear zones of the zonal wind QBO (see Figure 1). Below 22 hPa (~26 km), where the MLS temperatures are based on NCEP analysis, we observe a weaker amplitude temperature QBO. This agrees with the results of *Fleming and Chandra* [1989], who showed that derived zonal winds from NCEP geopotential heights produce a weaker amplitude QBO compared with radiosonde observations. Based on the observed shear zones of the zonal wind QBO, we expect the temperature QBO to extend down to altitudes below 20 km. Above 35 km, the SAO is evident. Cold anomalies at the solstices correspond to the easterly phase of the SAO and warm anomalies at the equinoxes correspond to the westerly SAO phase. As with the zonal wind data, the QBO region above 35 km is modulated by the SAO.

The MLS temperature power spectra (Figure 3) show significant amplitudes in the QBO frequency between 25 and 40 km. A maximum QBO amplitude of 1.8 K is reached at 27 km,

where the QBO frequency explains about 38% of the variability in the time series. Between 30 and 37 km, weaker amplitudes from 1.0 K to 1.3 K are observed. This is in approximate agreement with previous observations of the temperature QBO, which showed amplitudes from 2 to 3 K between 25 and 35 km and 1 to 2 K between 35 and 45 km [*Nastrom and Belmont*, 1975]. The annual cycle has amplitudes of 0.9 K between 18 and 21 km and 0.6 to 0.8 K between 34 and 48 km, with weaker contributions at intermediate altitudes. The amplitude of the semiannual period increases from 0.6 K at 32 km to 1.5 K at 42 km. This agrees with the results of *Ray et al.* [1994], who examined the first 18 months of MLS data for SAO signals.

The temperature time series can be reconstructed using only the QBO frequency to determine the phase relationship between temperatures at different altitudes. Plate 1 shows the reconstructed data using only the 27-month Fourier component superimposed on the MLS observations. There is good overall agreement between the reconstructed time series and the observations, although the amplitude of the reconstructed field is somewhat weaker than observations. The weaker amplitude is simply a result of other time variations (e.g., annual and semiannual) in the temperature data as seen in Figure 3. Between 23 and 30 km, the QBO is the dominant mode of variability, with a maximum amplitude in the QBO signal of 1.2 K at 27 km. From 30 to 45 km, the alternating warm and cold anomalies of the SAO are continuously observed but appear to be modulated by the QBO. For example, at 37 km, during the cold phase of the QBO, cold anomalies of the SAO (present at solstices) are larger and persist longer than warm anomalies, while during warm phases of the QBO, warm SAO anomalies have larger amplitudes and persist longer than cold anomalies. Between 27 and 37 km, the temperature anomaly descends at a rate of about 0.9 km/month, in approximate agreement with descent rates of the zonal wind QBO as observed by HRDI. Below 27 km, the QBO temperature signal is weaker and descends at a faster rate. The presence of a QBO signal from 20 to 45 km has also been reported by *Hamiliton* [1981] who examined rocketsonde data from Ascension island between 1967 and 1972.

4. Influence of the QBO on Constituent Fields

The power spectra for HALOE CH_4 and HF time series between 4°S and 4°N are shown in Figure 4. Both spectra show little variability from 20 to 30 km. Large-amplitude HF signals below 23 km have been attributed to sunspot contamination or data artifacts by *Russell et al.* [1996]. Between 35 and 45 km, there are large QBO amplitudes in both CH_4 and HF power spectra, with weaker semiannual and annual components also present. The peak QBO amplitude of 0.06 ppmv (0.04 ppbv) for CH_4 (HF) is found at 40 km. Plate 2 shows the observed time series for HF and CH_4 with the QBO reconstructed data superimposed with the black contours. Again, the comparison between the reconstructed data and the observations provides a visual check as to how well the QBO represents the observations. Clearly evident are periods when the QBO modulates the annual and semiannual variations. For example, in 1993 the low-concentration phase of the CH_4 QBO is interrupted by the annually varying cycle during January 1994. A comparison between CH_4 and HF anomalies shows an out of phase relationship above 30 km. This is expected as a result of the QBO-induced vertical velocity field acting on the oppositely orientated vertical gradients of CH_4 and HF. The high level of agreement in anticorrelation between HF and CH_4 anomalies
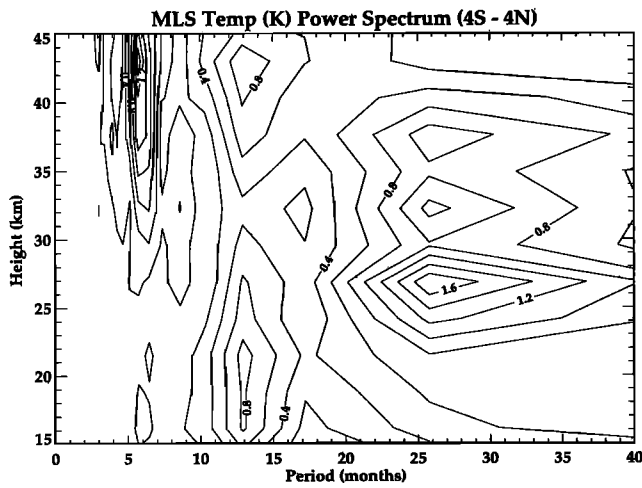
Figure 3. Amplitude of the MLS temperature power spectra from 4°S to 4°N. Contour intervals are 0.2 K.
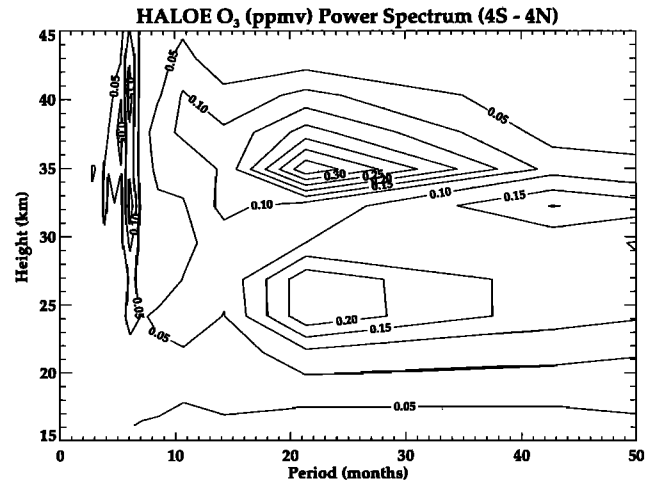

Figure 5. Amplitude of the HALOE power spectra for O_3 between 4°S and 4°N. Contour intervals are 0.1 ppmv.

in the tropics has also been observed in the midlatitudes [*Luo et al.*, 1994] and provides additional confidence in the quality of this UARS data.

HALOE O_3 power spectra and data reconstruction using

Figure 4. Amplitude of the HALOE power spectra for (a) CH_4 and (b) HF between 4°S and 4°N. Contour intervals are 0.01 ppmv for CH_4 and 0.01 ppbv for HF.

only the QBO frequency are shown in Figure 5 and Plate 3. In the power spectra the amplitude of the QBO frequency has two peaks, at 27 and 36 km in altitude. At 27 km, ozone is primarily under dynamical control and thus appears roughly in phase with the temperature anomaly. The cold anomaly in late 1993 (at 27 km) is associated with upward motion bringing low ozone anomalies to higher altitudes. Above 30 km in the tropics, ozone is largely under photochemical control and responds rapidly to temperature variations. Therefore, at the QBO maximum at 36 km, ozone and temperature are out of phase. The variations in ozone above 30 km resemble the variations seen in the temperature data; the observed SAO appears to be modulated by the QBO.

For CH_4 and HF the presence of a strong QBO signal only above 35 km may be explained by considering the vertical gradients of the constituent fields. Because the tropics are believed to be mostly isolated from the rapid mixing of the midlatitudes, especially between 20 and 28 km [*Schoeberl et al.*, 1997], tropical constituent profiles should therefore remain relatively undisturbed from horizontal transport influences [*Plumb*, 1996; *Avallone and Prather*, 1996]. If this is true, then the slow chemical production/destruction time- scales of CH_4 and HF in the lower stratosphere coupled with the slow mean ascent rate of the tropical stratosphere should produce constituent profiles with weak vertical gradients at these altitudes.

Average vertical profiles of HALOE CH_4 and HF taken from April 1992 through June 1996 in the tropics and midlatitudes are shown in Figure 6. Note that the vertical gradients of CH_4 and HF are maintained through photochemical reactions. Clearly apparent below 30 km is the weaker vertical gradients in CH_4 and HF profiles in the tropics compared with the midlatitudes. Also evident in the tropical constituent data is the sharp difference in the vertical constituent gradients between the lower and upper stratosphere. For example, the vertical gradient of tropical CH_4 between 30 and 40 km is almost twice as large as the gradient between 20 and 30 km. Average gradients in tropical HF are more than 3 times as large in the 30-40 km range compared with altitudes between 20 and 30 km. Because vertical transport is the product of the vertical motion field and the vertical constituent gradient (e.g., $Wd\chi/dz$), and because the QBO-induced vertical motion fields do not vary greatly from 20 to 40 km, we would therefore expect the
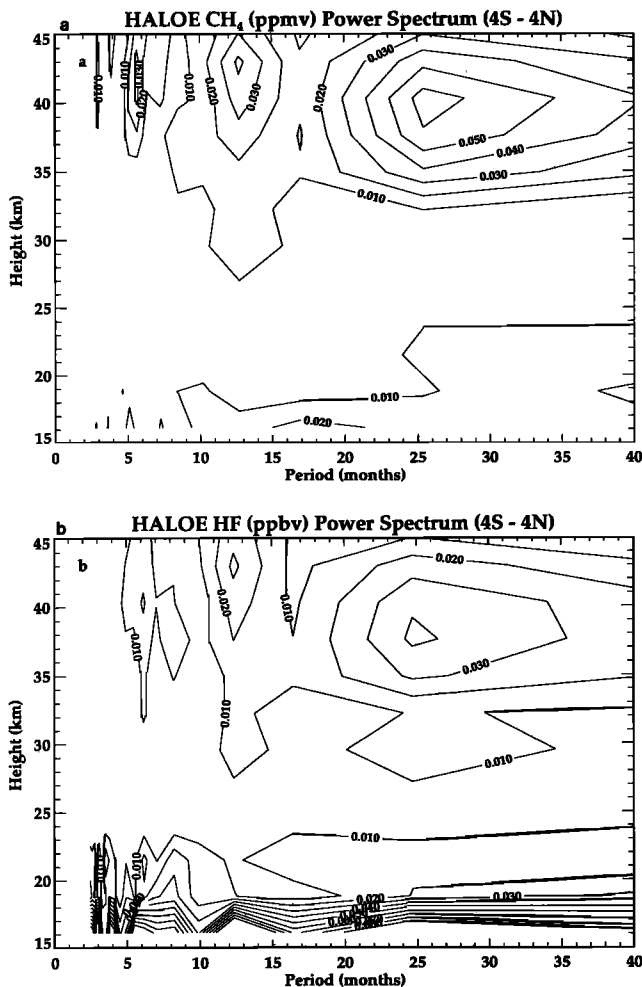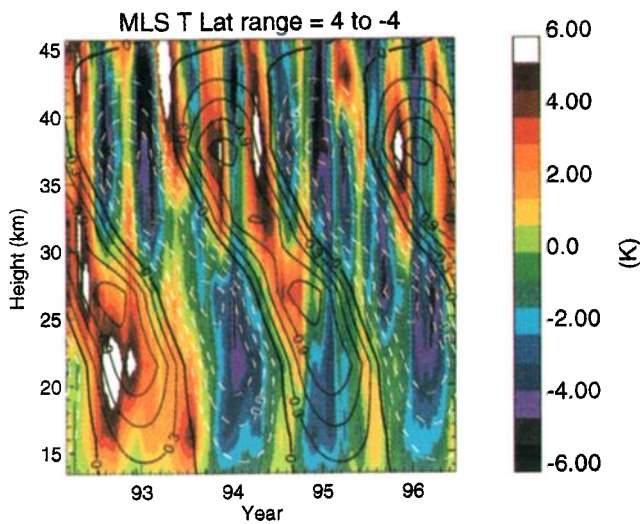
Plate 1. Time-height cross section of MLS temperature anomalies between 4°S and 4°N (colors). Superimposed on the MLS temperature data is the reconstructed temperature data using only the QBO frequency from the Fourier analysis. Black contours denote positive values, white (dashed) contours denote negative values. Contour intervals are 0.3 K.
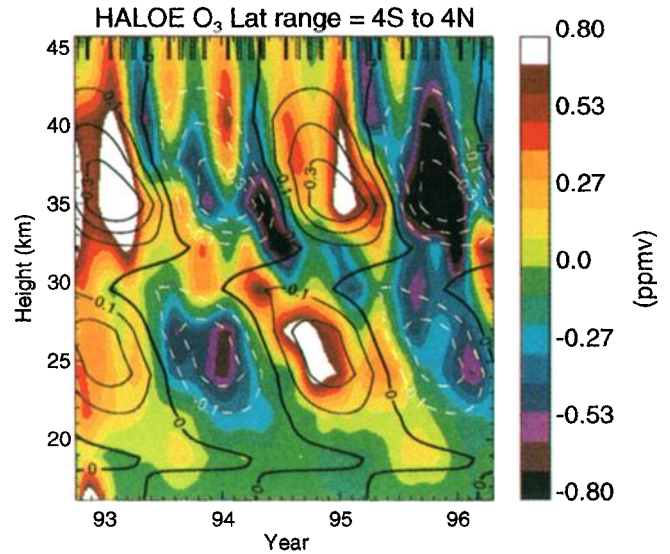

Plate 3. As in Plate 2 except for HALOE O_3. Contour interval is 0.1 ppmv for the reconstructed data.

maximum QBO signals in CH_4 and HF to appear where the vertical gradients are largest. Thus, in the tropics, observations show the largest CH_4 and HF QBO signals above 35 km, where constituent gradients are largest, and small CH_4 and HF QBO signals below 35 km, where constituent gradients are weak. A similar situation is also observed with the ozone data. In the dynamically controlled region, sharp vertical constituent gradients located below the ozone peak between 25 and 30 km are collocated with the large QBO amplitudes. Therefore analysis of constituent QBO signals should consider the natural constituent gradient as an important indicator for determining at what altitude the QBO signals will be present.
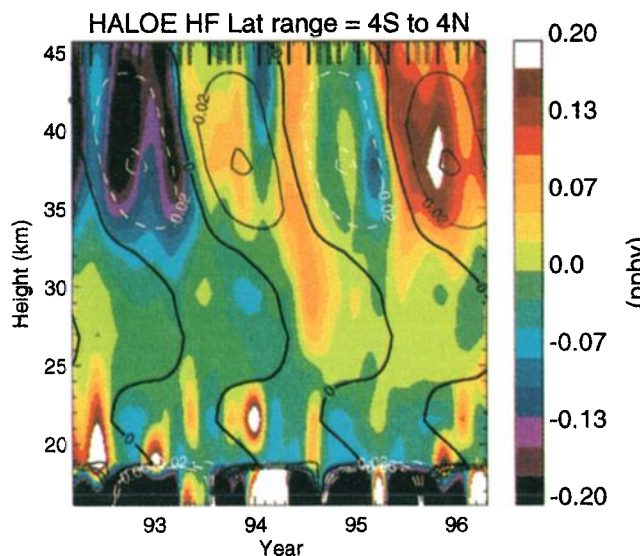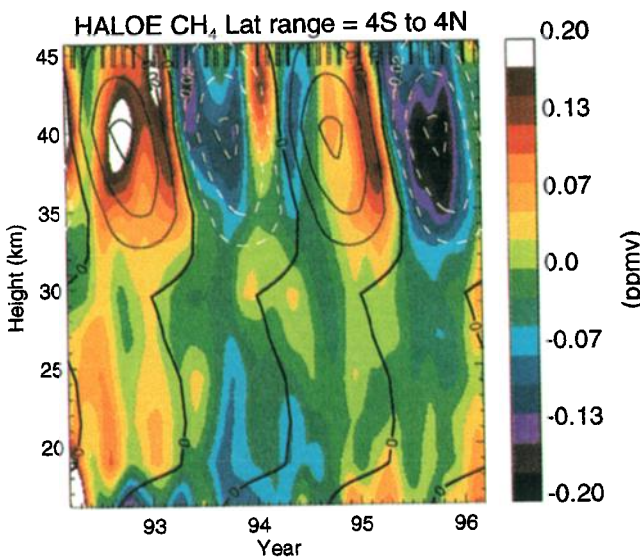
5. QBO Transport Model

We employ a simple model of vertical transport in the tropics to better understand the UARS observations. By assuming that the tropics remain relatively isolated from the midlatitudes, a one-dimensional (1-D) vertical transport model using parameterized chemistry can be used to simulate the variability of tropical constituents [*Avallone and Prather*, 1996; *Schoeberl et al.*, 1997]. In the model, HRDI winds are used to specify the vertical wind shear (u_z); thus chemical and dynamical processes can be assessed by comparing model output with observations.

The model is constructed with the following assumptions: the timescale of the QBO is long compared with seasonal variations; the QBO wind oscillation is nearly symmetric about the equator; and the thermal wind relationship remains valid even near the equator [*Andrews et al.*, 1987]. Using an equatorial beta-plane model, the thermal wind, thermodynamic energy, and constituent continuity equation, respectively, are given as [*Hasebe*, 1994]

Plate 2. HALOE observed CH_4 and HF anomalies averaged between 4°S and 4°N. Time means have been removed. Contour represents the reconstructed time series using only the QBO frequency. Black contours denote positive values; white (dashed) contours denote negative values. Contour intervals are 0.02 ppmv for CH_4 and 0.02 ppbv for HF. Tick marks on the upper abscissa indicate the HALOE measurement times.
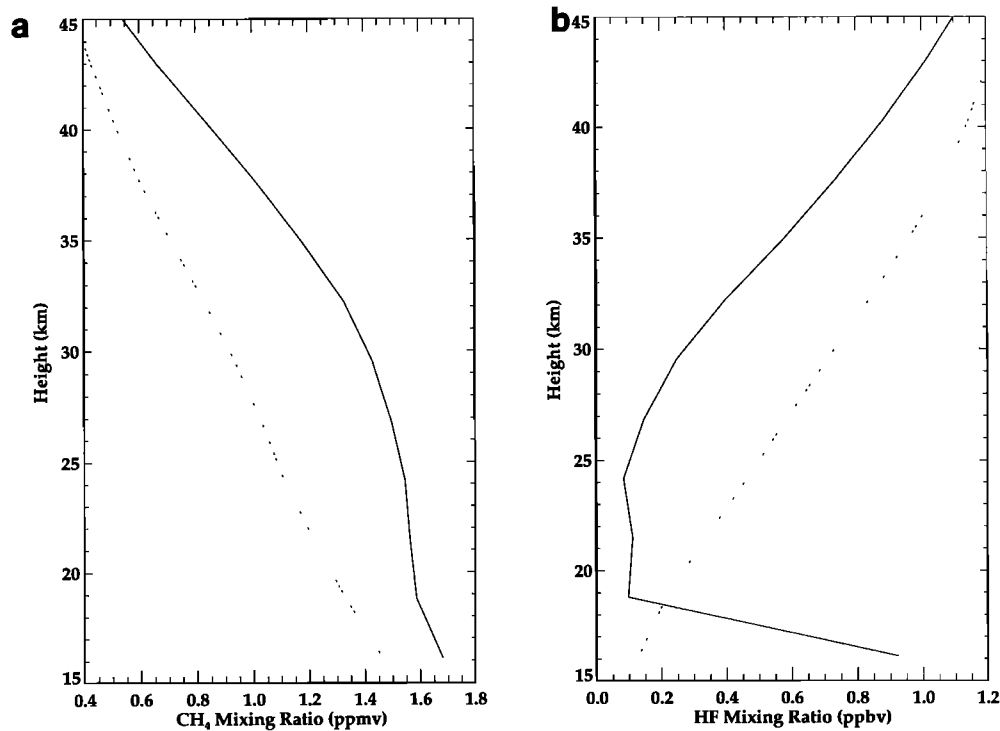
Figure 6. Average (a) CH_4 and (b) HF profiles from HALOE from April 1992 to June 1996. Solid lines represent tropical averages (4°S to 4°N), and dotted lines represent midlatitude averages (40°N to 50°N).

$$d(U_q)/ dz = -(R/(H\beta y))d(T_q)/ dy \qquad (1)$$

$$N^2 W_q = -(\alpha R T_q)/H \qquad (2)$$

$$d(\chi_m) / dt + (W_m + W_q)d(\chi_m)/ dz = - K_{chem}\chi_m \qquad (3)$$

where the subscript q denotes the QBO component and m denotes the mean component. The Newtonian cooling coefficient, $\alpha(z)$, is taken from the slow damping profiles of *Dunkerton* [1979], and K_{chem} is the chemical production/loss rates of the constituent χ_m. The other atmospheric variables are defined in Table 1.

Equations (1) and (2) are solved by specifying the zonal wind field from observations and then diagnostically determining the temperature and QBO-induced vertical motion. The HRDI zonal winds from January 1992 through June 1996 at the equator are interpolated in time to force the model toward

Table 1. List of Symbols

Symbol	Definition
$x, y, z = -H \ln(p/p_0)$	eastward, northward, and vertical direction
p_0	sea level reference pressure, equal to 1000 hPa
H	scale height, equal to 7 km
β	northward gradient of Coriolis parameter evaluated at the equator, equal to 2.29 x 10^{-11} m^{-1}s^{-1}
$N^2T)$	Brünt Väisälä frequency squared
R	dry air gas constant, equal to 287 J K^{-1} kg^{-1}
Ω	Earth's rotation rate
a	Earth's radius
$K_{chem}(z)$	chemical relaxation rate
U, W	zonal and vertical velocities
$\alpha(z)$	Newtonian cooling coefficient

observations. From (1), the QBO-induced temperature anomaly is evaluated as $T_q = L^2 H \beta R^{-1} u_z$ [*Andrews et al.*, 1987], where L (~1500 km) is the meridional scale of the QBO [*Hasebe*, 1994], and H, R, and β are defined in Table 1. The choice of the QBO meridional scale, L, produced reasonable agreement between the calculated temperature anomaly and that observed by MLS. Assuming we know the production/ loss of the chemical constituent χ_m, the remaining unknown in (3) is the mean vertical motion field (W_m). This quantity clearly has an important impact on long lived tracers. For example, CH_4, which has no mechanism for production in the stratosphere, enters the stratosphere at about 1.7 ppmv. Because the chemical loss of CH_4 is dependent on residence time, a stronger vertical ascent rate would mean less chemical loss of methane and thus a greater mixing ratio at higher altitudes. The situation for HF is similar except that its vertical gradient has the opposite sign in the stratosphere. After specifying the vertical ascent rate in the tropics, model constituent concentrations can then be compared with observations.

One-dimensional vertical transport models of the lowest levels of the tropical stratosphere have assumed a constant mean vertical motion field [*Avallone and Prather*, 1996; *Minschwaner et al.*, 1996]. At higher levels of the stratosphere where the QBO is important, however, the mean ascent rate in the tropics varies with height and season [*Rosenfield et al.*, 1987; *Rosenlof and Holton*, 1993].

In the model experiments presented here, we will consider both constant and variable vertical motion rates and use CH_4 as our model constituent. CH_4 loss rates which vary with latitude, height, and season are obtained from the two-dimensional (2-D) Goddard model [*Jackman et al.*, 1997], and initial conditions are determined from average HALOE tropical profiles. In the first experiment, the mean vertical motion field is set to a constant value of 0.04 km/d, the largest ascent rate used by

Avallone and Prather [1996]. In the second experiment, W_m from the Goddard 2-D model, which has latitude, height, and temporal variation, is interpolated into the model domain. The Goddard 2-D model output is a climatology; thus the vertical motion field contains annual variation but no interannual variations.

Plate 4 (top panel) shows the time series of the CH_4 anomaly (time mean subtracted out) at the equator from the 1-D model.
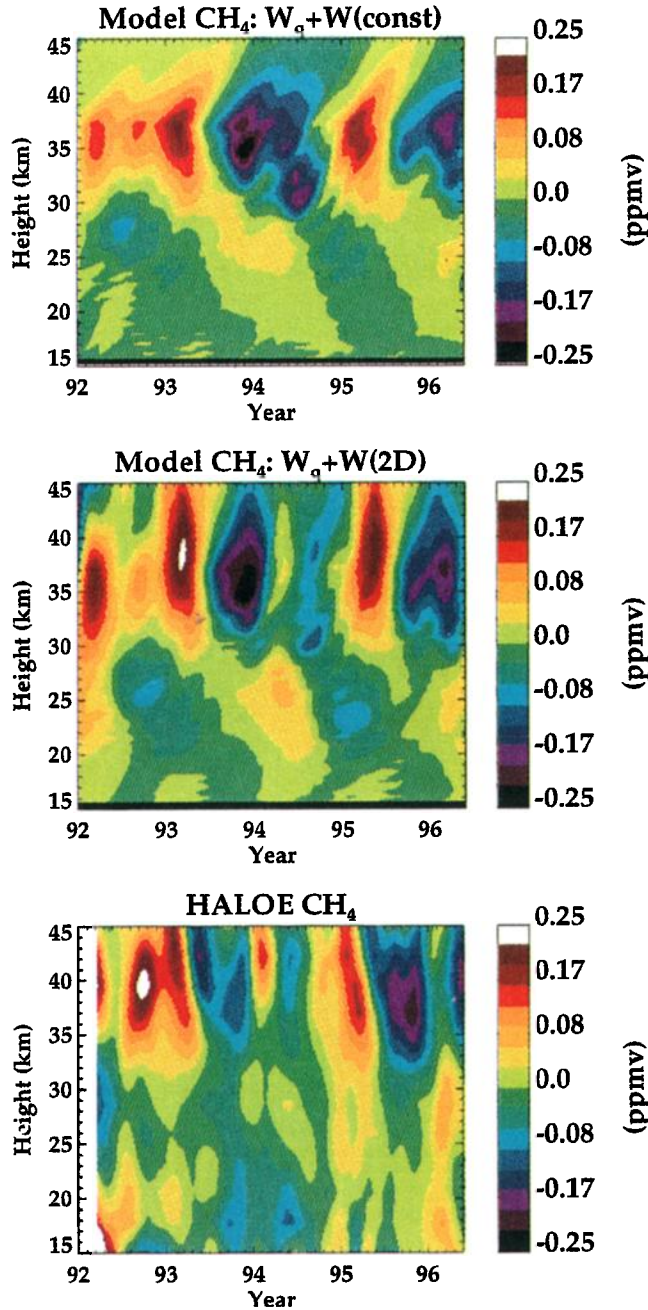
Model CH₄: Wₐ+W(const)

Model CH₄: Wₐ+W(2D)

HALOE CH₄

Plate 4. Time-height plots of CH_4 anomaly at the equator from the 1-D model. Time means have been removed. (top) Model-calculated CH_4 using QBO-induced vertical velocities and a constant mean ascent rate (W_m=0.04 km/d). (middle) Model-calculated CH_4 using QBO-induced vertical velocities and a seasonally varying ascent rate (W_m from the NASA Goddard 2-D model). (bottom) Observed CH_4 anomaly from HALOE. Black heavy contour represents the zero line.
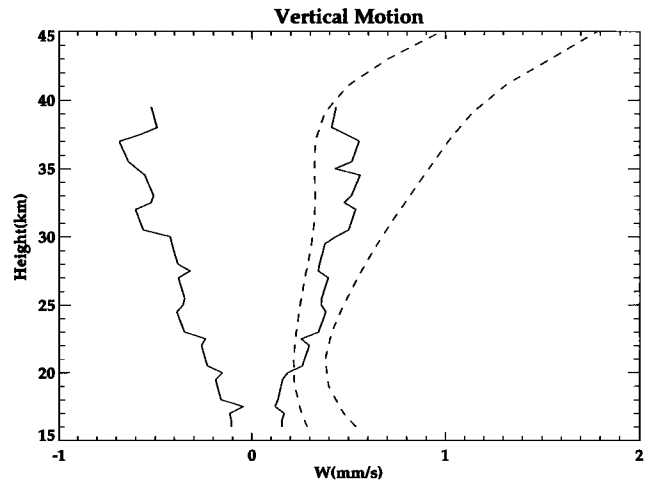
Vertical Motion

Figure 7. Vertical motion fields used in the 1-D model. Solid lines represent the minimum and maximum vertical motions induced by the QBO as calculated from the HRDI zonal winds. Dashed lines represent the minimum and maximum vertical motion fields from the Goddard 2-D model. Note that QBO-induced vertical motion above 40 km is not plotted because there are no HRDI winds available.

The vertical motion field is composed of a QBO portion, calculated diagnostically from the HRDI winds, plus a constant value (W_m= 0.04 km/d), which represents the mean vertical ascent rate in the tropics. Below 30 km, there is little variation in the constituent field, while between 35 and 45 km, anomalies in CH_4 of ± 0.2 ppmv are present. Comparisons with the HALOE observations (Plate 4, bottom panel) above 35 km show a similarity in the large-scale features, although there are also considerable differences. For example, although there is good correspondence between the level at which variations are maximum (35-40 km), shorter period oscillations in the observations (a year or less) are absent in the model simulation. In addition, the absolute magnitude of the model CH_4 is 5-15% lower than the HALOE observations (not shown). This indicates that either the model vertical motion field is too weak or that there is some contributions from horizontal mixing of CH_4 between the midlatitudes and the tropics. The phase difference between the model and observations above 35 km is another indication of a vertical motion field that is too small.

Plate 4 (center panel) shows the results from experiment 2, where the residual motion field (W_m) from the Goddard 2-D model is used. Because the 2-D model has a seasonal variation in the tropical ascent rate, the model CH_4 anomaly possess an annual, semiannual, and QBO variation above 30 km. Agreement with observations is significantly improved. In particular, note how in early 1994, the low CH_4 anomaly is interrupted by a high anomaly between 30 and 40 km. The combination of the QBO and the seasonal variations appears to explain most of the variability in the HALOE time series. However, the HALOE observations do show some variation below 30 km. The sources of this may be due to tropical/midlatitude exchange which is not accounted for in this model.

A comparison of the vertical motion fields used in the model are shown in Fig 7. The solid lines represent the minimum and maximum vertical motion rates due to the QBO, as calculated from (2). The dashed lines represent the minimum and maxi-

mum vertical ascent rates (April 10 and January 1, respectively) obtained from the Goddard 2-D model at the equator. The QBO-induced vertical velocities are only representative of periods during maximum vertical wind shears; more typical vertical motion fields due to the QBO range from -0.3 to 0.2 mm/s between 23 and 37 km in altitude. Even so, the QBO-induced vertical motions are still an important component of the tropical circulation. For example, inspection of the total vertical motion field ($Wq + W_m$; not shown) reveals periods (1-2 months) when there is weak downward motion in the lower tropical stratosphere (25-35 km). These events occurred during equinoxes in 1992 and 1994, when the downward motion associated with strong westerly shear zones overcame the weaker upward motions of the equinox. Evidence of very weak or negative tropical ascent rates can also be identified from HALOE observations of water vapor (H_2O) at the equator [*Schoeberl et al.*, 1997]. The ascending H_2O anomalies are disturbed from their diabatic circulation by the shear zones of the QBO [*Mote et al.*, 1996, *Schoeberl et al.*, 1997]. This is particularly evident during the middle of 1994, when strong westerly shear zones appear to delay the upward propagating H_2O field by up to 3 months. We also note that the apparent lack of symmetry between the QBO induced upward and downward motion is in agreement with the notion that the westerly shear zones are stronger than the easterly shear zones.

Interannual variability in tropical ascent rates also appears to play a role in tropical constituent transport. The existence of a stronger tropical ascent rate during January is expected by the increased planetary wave activity during the northern hemisphere winter [*Randel*, 1992]. The model results from experiment 2 show that during successive Januarys, positive anomalies in CH_4 are present above 30 km. However, in January 1994, the positive anomaly is very weak due to the strong negative anomaly induced by the QBO. Inspection of the HALOE observations shows that a positive anomaly should be present during this time. A much better agreement between the model and observations is made by increasing W_m from the 2-D model by 30% during the winter of 1994 (not shown), a reflection of the observed interannual variations in the tropical mean ascent rate [e.g., *Randel*, 1992]. In fact, this interannual variability in the tropical ascent rate may be in part due to the tropical QBO. A number of studies have indicated the sensitivity of extratropical wave activity to the phase of tropical zonal wind QBO [*O'Sullivan and Salby*, 1990; *O'Sullivan and Chen*, 1996]. If interannual variability in extratropical wave activity is linked to the QBO, then tropical ascent rates should also possess this variability.

6. Conclusions

An analysis of UARS data from 1991 through mid-1996 has been used to study the variability of long-lived tracers in the tropical stratosphere. HRDI zonal wind data reveal that during the UARS period, the equatorial QBO had an amplitude of 20 m/s and a period of about 27 months between 20 and 40 km in altitude. A corresponding temperature QBO with an amplitude of about 2 K is observed by MLS. Power spectra analysis of the zonal wind data shows the dominant QBO frequency is maximized at 27 km. Power spectra of MLS temperature data show significant amplitude in the QBO frequency between 27 and 37 km, and even larger amplitudes in the semiannual frequency between 35 and 45 km. The temperature observations indicate that below 30 km, the QBO is the dominant mode of

variability, while between 35 and 45 km, although the QBO is still present, it is modified by the SAO.

HALOE observations of CH_4, HF and O_3 between 4°S and 4°N are also studied using a power spectrum analysis. Both CH_4 and HF time series indicate a strong QBO signal from 35 to 45 km, with weak signals at lower altitudes. O_3 has a strong QBO signal at 27 and 36 km. The variability of CH_4, HF, and O_3 (in the lower stratosphere) is related to both the magnitude of the vertical motion field and the vertical constituent gradient. Thus, because CH_4 and HF have weak vertical gradients below 30 km and sharper gradients between 35 and 45 km, the QBO signals are only seen above 35 km. In the lower stratosphere, O_3 gradients are sharp, thus QBO signals are also present. In the upper stratosphere, O_3 is under photochemical control and is thus unaffected by dynamical variations. For both HF and CH_4 the QBO variations are modified by an annual or semiannual component above 35 km.

A simple 1-D vertical transport model constrained by HRDI zonal wind observations is used to further explore constituent transport in the tropical stratosphere. Model results confirm that both annual and interannual (e.g., QBO) variations in the vertical motion field are important for transport between 30 and 45 km in the deep tropics. The vertical motion associated with the strong shear zones of the QBO are found to significantly modify the annually varying tropical ascent rate. Because of the good correspondence between the model and observations, the model vertical motion field should provide a reasonable estimate of the true ascent rates in the tropics. These rates can then be compared with global models to access their accuracy in simulating transport in the tropical stratosphere.

The results of this study indicate that QBO signals in long-lived tracers may exist between 20-45 km, depending upon the altitude and vertical constituent gradient. Below 30 km, the QBO-induced vertical velocities can be as large as the mean ascent rate; thus QBO signals should be strong if there are significant vertical constituent gradients. Above 35 km, the annually varying mean ascent rate is also important and will modify the QBO signal. The QBO amplitude appears to diminish above 45 km.

Although this study has focused on the QBO's influence on vertical transport in the deep tropics, the influence of the QBO on meridional transport both in the tropics and subtropics can also be investigated with the UARS data. A better understanding of the annual and interannual variability of meridional and vertical transport in the tropics is important for evaluating and improving transport in global models. This work is currently ongoing and will be reported in a future paper.

References

Andrews, D. G., J. R. Holton, and C. B. Leovy, *Middle Atmosphere Dynamics*, 498 pp., Academic, San Diego, Calif., 1987.

Angell, J. K., and J. Korshover, Quasi-biennial, annual and semiannual zonal wind and temperature harmonic amplitudes in the stratosphere and low mesosphere of the northern hemisphere, *J. Geophys. Res.*, 75, 543-550, 1970.

Angell, J. K., and J. Korshover, Quasi-biennial and long-term fluctuations in total ozone, *Mon. Weather Rev.*, 101, 426-443, 1973.

Avallone, L., and M. Prather, Photochemical evolution of ozone in the lower tropical stratosphere, *J. Geophys. Res.*, *101*, 1457-1461, 1996.

Brühl, C., S. R. Drayson, J. M. Russell III, P. J. Crutzen, J. M. McInerney, P. N. Purcell, H. Claude, H. Gernandt, T. J. McGee, I. S. McDermid, and M. R. Gunson, Halogen Occultation Experiment ozone channel validation, *J. Geophys. Res.*, *101*, 10,217-10,240, 1996.

Chipperfield, M. P., L. J. Gray, J. S. Kinnersley and J. Zawodny, A two-dimensional model study of the QBO signal in SAGE II NO₂ and O₃, *Geophys. Res. Lett.*, *21*, 589-592, 1994.

Dunkerton, T., On the role of the Kelvin wave in the westerly phase of the semiannual zonal wind oscillation, *J. Atmos. Sci.*, *36*, 32-41, 1979.

Dunkerton, T. J., A two-dimensional model of the quasi-biennial oscillation, *J. Atmos. Sci.*, *42*, 1151-1160, 1985.

Dunkerton, T. J., and D. P. Delisi, Climatology of the equatorial lower stratosphere, *J. Atmos. Sci.*, *42*, 376-396, 1985.

Fishbein, E. F., et al., Validation of UARS Microwave Limb Sounder temperature and pressure measurements, *J. Geophys. Res.*, *101*, 9983-10,016, 1996.

Fleming, E. L., and S. Chandra, Equatorial zonal wind in the middle atmosphere derived from geopotential height and temperature data, *J. Atmos. Sci.*, *46*, 860-866, 1989.

Funk, J. P., and G. L. Garnham, Australian ozone observations and a suggested 24-month cycle, *Tellus*, *14*, 378-382, 1962.

Hamiliton, K., The vertical structure of the quasi-biennial oscillation: Observations and theory, *Atmos. Ocean*, *19*, 236-250, 1981.

Hasebe, F., The global structure of the total ozone fluctuations observed on the time scales of two to several years, in *Dynamics of the Middle Atmosphere*, edited by J. R. Holton and T. Matsuno,, pp. 445-464, *Terra Sci.*, Tokyo, 1984.

Hasebe, F., Quasi-biennial oscillations of ozone and diabatic circulation in the equatorial stratosphere, *J. Atmos. Sci.*, *51*, 729-745, 1994.

Hervig, M. E., et al., Validation of temperature measurements from the Halogen Occultation Experiment, *J. Geophys. Res.*, *101*, 10,277-10,285, 1996.

Hollandsworth, S. M., K. P. Bowman, and R. D. McPeters, Observational study of the quasi-biennial oscillation in ozone, *J. Geophys. Res.*, *100*, 7347-7361, 1995.

Holton, J. R., and R. S. Lindzen, An updated theory for the quasi-biennial cycle of the tropical stratosphere, *J. Atmos. Sci.*, *29*, 1076-1080, 1972.

Jackman, C. H., E. L. Fleming, S. Chandra, D. B. Considine, and J. E. Rosenfield, Past, present, and future modeled ozone trends with comparisons to observed trends, *J. Geophys. Res.*,*101*, 28,753-28,767, 1997.

Lait, L. R., M. R. Schoeberl, and P. A. Newman, Quasi-biennial modulation of the Antarctic ozone depletion, *J. Geophys. Res.*, *94*, 11,559-11,571, 1989.

Lindzen, R. S., and J. R. Holton, A theory of the quasi-biennial oscillation, *J. Atmos. Sci.*, *49*, 785-801, 1968.

Ling, X.-D., and J. London, The quasi-biennial oscillation of ozone in the tropical middle atmosphere: A one-dimensional model, *J. Atmos. Sci.*, *43*, 3122-3137, 1986.

Luo, M., R. J. Cicerone, J. M. Russell III, and T. Huong, Observations of stratospheric hydrogen fluoride by the Halogen Occultation Experiment (HALOE), *J. Geophys. Res.*, *99*, 16,691-16,704, 1994.

Minschwaner, K., A. E. Dessler, J. W. Elkins, C. M. Volk, D. W. Fahey, M. Loewenstein, J. R. Podolske, A. E. Roche, and K. R. Chan, Bulk properties of isentropic mixing into the tropics in the lower stratosphere, *J. Geophys. Res.*, *101*, 9433-9439, 1996.

Mote, P. W., K. H. Rosenlof, M. E. McIntyre, E. S. Carr, J. C. Gille, J. R. Holton, J. S. Kinnersley, H. C. Pumphrey, J. M. Russell, and J. W. Waters, An atmospheric tape recorder: the imprint of tropical tropopause temperatures on stratospheric water vapor, *J. Geophys. Res.*, *101*, 3989-4006, 1996.

Nastrom, G. D., and A. D. Belmont, Periodic variation in stratospheric-mesospheric temperature from 20-65 km at 80 N to 30 S, *J. Atmos. Sci.*, *32*, 1715-1722, 1975.

Naujokat, B., An update of the observed quasi-biennial oscillation, *J. Atmos. Sci.*, *25*, 1095-1107, 1986.

Oltmans, S. J., and J. London, The quasi-biennial oscillation in atmospheric ozone, *J. Geophys. Res.*, *87*, 8981-8989, 1982.

Ortland, D. A., W. R. Skinner, P. B. Hays, M. D. Burrage, R. S. Lieberman, A. R. Marshall, and D. A. Gell, Measurements of stratospheric winds by the high resolution Doppler imager, *J. Geophys. Res.*, *101*, 10,351-10,363, 1996.

O'Sullivan, D., and P. Chen, Modeling the quasi-biennial oscillation's effect on the winter stratospheric circulation, *J. Geophys. Res.*, *101*, 2437-2448, 1996.

O'Sullivan, D., and M. L. Salby, Coupling of the quasi-biennial oscillation and the extratropical circulation in the stratosphere through planetary wave transport, *J. Atmos. Sci.*, *47*, 650-673, 1990.

Park, J. H., and J. M. Russell III, Summer polar chemistry observations in the stratosphere made by HALOE, *J. Atmos. Sci.*, *51*, 2903-2913, 1994.

Park, J. H., et al., Validation of Halogen Occultation Experiment CH₄ measurements from the UARS, *J. Geophys. Res.*, *101*, 10,183-10,203, 1996.

Plumb, R. A., A tropical pipe model of stratospheric transport, *J. Geophys. Res.*, *101*, 3957-3972, 1996.

Plumb, R. A., and R. C. Bell, A model of the quasi-biennial oscillation on an equatorial beta-plane, *Q. J. R. Meteorol. Soc.*, *108*, 335-352, 1982.

Randel, W. J., Global atmospheric circulation statistics, 1000-1 mb, *NCAR Tech. Note NCAR/TN-366 + STR*, 1992.

Randel, W. J., and F. Wu, Isolation of the ozone QBO in SAGE II data by singular-value decomposition, *J. Atmos. Sci.*, *53*, 2546-2559, 1996.

Ray, E. A., J. R. Holton, E. F. Fishbein, L. Froidevaux and J. W. Waters, The tropical semiannual oscillation in temperature and ozone as observed by the MLS, *J. Atmos. Sci.*, *51*, 3045-3052, 1994.

Reed, R. J., A tentative model of the 26-month oscillation in tropical latitudes, *Q. J. R. Meteorol. Soc.*, *90*, 441-466, 1964.

Reed, R. J., W. J. Campbell, L. A. Rasmussen, and D. G. Rogers, Evidence of downward propagating annual wind reversal in the equatorial stratosphere, *J. Geophys. Res.*, *66*, 813-818, 1961.

Rosenfield, J. E., M. R. Schoeberl, and M. A. Geller, A computation of the stratospheric diabatic circulation using an accurate radiative transfer model, *J. Atmos. Sci.*, *44*, 859-876, 1987.

Rosenlof, K. H., and J. R. Holton, Estimates of the stratospheric residual circulation using the downward control principle, *J. Geophys. Res.*, *98*, 10,465-10,479, 1993.

Russell, J. M., et al., Validation of hydrogen fluoride measurements made by the Halogen Occultation Experiment from the UARS platform, *J. Geophys. Res.*, *101*, 10,163-10,174, 1996.

Schoeberl, M. R., A. E. Roche, J. M. Russell III, D. Ortland, and P. B. Hays, An estimation of the dynamical isolation of the tropical lower stratosphere using UARS wind and trace gas observations of the quasi-biennial oscillation, *Geophys. Res. Lett.*, *24*, 53-57, 1997.

Takahashi, M., and B. A. Boville, A three-dimensional simulation of the equatorial quasi-biennial oscillation, *J. Atmos. Sci.*, *49*, 1020-1035, 1992.

Tung, K. K., and H. Yang, Global QBO in circulation and ozone. Part I.: Reexamination of observational evidence, *J. Atmos. Sci.*, *51*, 2699-2707, 1994.

Veryard, R. G., and R. A. Ebdon, Fluctuations in tropical stratospheric winds, *Meteorol. Mag.*, *90*, 125-143, 1961.

Zawodny, J. M., and M. P. McCormick, Stratospheric aerosol and gas experiment II measurements of the quasi-biennial oscillations in ozone and nitrogen dioxide, *J. Geophys. Res.*, *96*, 9371-9377, 1991.

E. C. Cordero, Universities Space Research Association, Atmospheric Chemistry and Dynamics, NASA Goddard Space Flight Center, Greenbelt, MD 20771. (e-mail: cordero@polska.gsfc.nasa.gov)

S. R. Kawa and M. R. Schoeberl, Laboratory for Atmospheres, NASA Goddard Space Flight Center, Greenbelt, MD 20771.